Increasing Multiyear Sea Ice Loss in the Beaufort Sea: A New Export Pathway for the Diminishing Multiyear Ice Cover of the Arctic Ocean

David G. Babb[1] (david.babb@umanitoba.ca) (ORCID: 0000- 0002-7427-8094)
Ryan J. Galley[2, 3] (ORCID: 0000-0002-5403-9694)
Stephen E.L. Howell[4] (ORCID: 0000-0002-4848-9867)
Jack C. Landy[5] (ORCID: 0000-0002-7372-1007)
Julienne C. Stroeve[1, 6, 7] (ORCID: 0000-0001-7316-8320)
David G. Barber[1] (ORCID: 0000-0001-9466-329)

[1] Centre for Earth Observation Science, University of Manitoba, Winnipeg, MB, Canada
[2] Department of Environment and Geography, University of Manitoba, Winnipeg, MB, Canada
[3] Department of Fisheries and Oceans Canada, Winnipeg, MB, Canada.
[4] Environment and Climate Change Canada, Toronto, ON, Canada
[5] Department of Physics and Technology, UiT The Arctic University of Norway, 9037 Tromsø, Norway;
[6] CPOM, London, United Kingdom
[7] NSIDC, Boulder, Colorado, United States

Keywords:

Sea ice; Multiyear ice; Beaufort Sea; Arctic Ocean; Sea ice dynamics; Beaufort Gyre

Key Points:

1. MYI area loss in the Beaufort Sea quadrupled from 46,000 km^2 yr^{-1} in 1997-2001 to 183,000 km^2 yr^{-1} in 2017-2021.
2. MYI area loss peaked at 385,000 km^2 in 2018, which is close to the annual MYI area export through Fram Strait.
3. The Beaufort Sea has become a MYI export pathway rivaling Fram Strait, encouraging the transition to a seasonal Arctic sea ice cover.

Abstract:

Historically multiyear sea ice (MYI) covered a majority of the Arctic and circulated through the Beaufort Gyre for years. However, increased ice melt in the Beaufort Sea during the early-2000s was proposed to have severed this circulation. Constructing a regional MYI budget from 1997-2021 reveals that MYI import into the Beaufort Sea has increased year-round, yet less MYI now survives through summer and is transported onwards in the Gyre. Annual average MYI loss quadrupled over the study period and increased from ~7% to ~33% of annual Fram Strait MYI export, while the peak in 2018 (385,000 km^2) was similar to Fram Strait MYI export. An accelerating ice-albedo feedback coupled with dynamic conditioning towards younger thinner MYI is responsible for the increased MYI loss. MYI transport through the Beaufort Gyre has not been severed, but it has been reduced so severely to prevent it from being redistributed throughout the Arctic Ocean.

Plain Language Summary:

Historically sea ice grew thicker and aged into multiyear sea ice (MYI) as it was transported clockwise around the Beaufort Gyre for up to and beyond 10 years. This pattern facilitated the pan-Arctic distribution of MYI that was typical of the 1980s and 1990s. However, warming temperatures and greater sea ice melt in the Beaufort Sea since the early 2000s has significantly increased the annual area of MYI lost to melt, and was proposed to have severed MYI transport through the Beaufort Gyre. Here we use a regional MYI budget to show that an increasing area of MYI is lost annually in the Beaufort Sea and that this has considerably altered and interrupted MYI transport through the Gyre for prolonged periods during recent years. This change has implications regionally for wildlife, shipping, and local communities, while also having an affect on the resiliency of the pan-Arctic ice pack.

1. Introduction:

Multiyear sea ice (MYI) comprises the thickest and most robust sea ice in the Arctic, however its extent is declining as the Arctic transitions to a predominantly seasonal ice cover (Kwok, 2018). Historically, MYI covered the vast majority of the Arctic (~5.5 x 10^6 km^2; Nghiem et al., 2007) and grew thicker as it circulated through the anticyclonic Beaufort Gyre for up to and beyond 10 years (Rigor & Wallace, 2004). In particular, years with a strong Beaufort Gyre (associated with the negative phase of the Arctic Oscillation (AO)) were generally conservative of MYI as they promoted MYI redistribution and limited ice export through Fram Strait (Rigor & Wallace, 2002; Stroeve et al., 2011). Within the Gyre, MYI is transported from the central Arctic, where the thickest and oldest ice is compressed against the northern coast of Greenland and the Canadian Arctic Archipelago (CAA; Bourke & Garret, 1987; Kwok, 2015), through the Beaufort Sea and on to the Eastern Arctic (Figure 1). The Beaufort Sea has therefore served as a conduit connecting the central Arctic to the Eastern Arctic and maintained the pan-Arctic distribution of MYI that was prevalent through the 1980s, 1990s and early 2000s (Maslanik et al., 2011). Critical to its role as a MYI conduit was the fact that from 1981-2005, 93% of MYI in the Beaufort Sea survived through summer (Maslanik et al., 2011).

Anomalous atmospheric forcing and record ice-loss during 1998 started the transition of the Beaufort ice pack to a thinner state (Hutchings & Rigor, 2012; Maslanik et al., 1999), and simultaneously sea ice melt, particularly bottom melt, increased in the early 2000s due to enhanced solar heating of the upper ocean (Perovich et al., 2008, 2011; Planck et al., 2020). In particular, Perovich et al., (2008) observed over 2 m of bottom melt on a 3 m thick MYI floe during summer 2007. This was six times greater than the mean value of bottom melt recorded in the 1990's and was attributed to anomalous solar heating of the upper ocean. Increased melt led to a reduction in MYI thickness from 2003-2012 (Krishfield et al., 2014), and an increase in MYI loss within the Beaufort Sea from 2000 through to a peak in 2008 (Kwok & Cunningham, 2010). Ultimately, the survival rate of MYI passing through the Beaufort Sea decreased to 73% from 2006-2010 (Maslanik et al., 2011), a change that was further emphasized by the complete loss of the regional MYI pack during summers 2010, 2012 and 2016 (Babb et al., 2016, 2019; Stroeve et al., 2011). However, regardless of MYI loss during summer, the Beaufort Sea has continued to be resupplied with MYI from the central Arctic via the Gyre (Babb et al., 2020; Galley et al., 2016; Howell et al., 2016), though less and less of it is likely to survive through summer and as a result younger ice has been exported across the western gate of the Beaufort Sea (Howell et al., 2016). This has led to younger ice recirculating within the Gyre (Hutchings & Rigor, 2012) and all but eliminated the supply of MYI to the Eastern Arctic which has been a predominantly seasonal ice cover since the mid-2000s (Nghiem et al., 2006).

Based on the increase in MYI loss in the Beaufort Sea during the early-2000s Maslanik et al. (2007) proposed that the previously continuous journey of MYI through the Beaufort Gyre had been severed and that the western Arctic had become an area of MYI export. In this paper we use 25 years of Canadian Ice Service (CIS) ice charts to present a MYI budget for the Beaufort Sea that accounts for MYI transport and quantifies the annual area of MYI lost to melt in the region from 1997 to 2021. We then examine the thermodynamic forcing and dynamic conditioning that is driving the increase in MYI loss and examine MYI loss in the Beaufort Sea relative to MYI export through other pathways. Ultimately, we examine whether MYI transport through the Beaufort Gyre has been severed, leaving the Beaufort Sea as an area of MYI export.

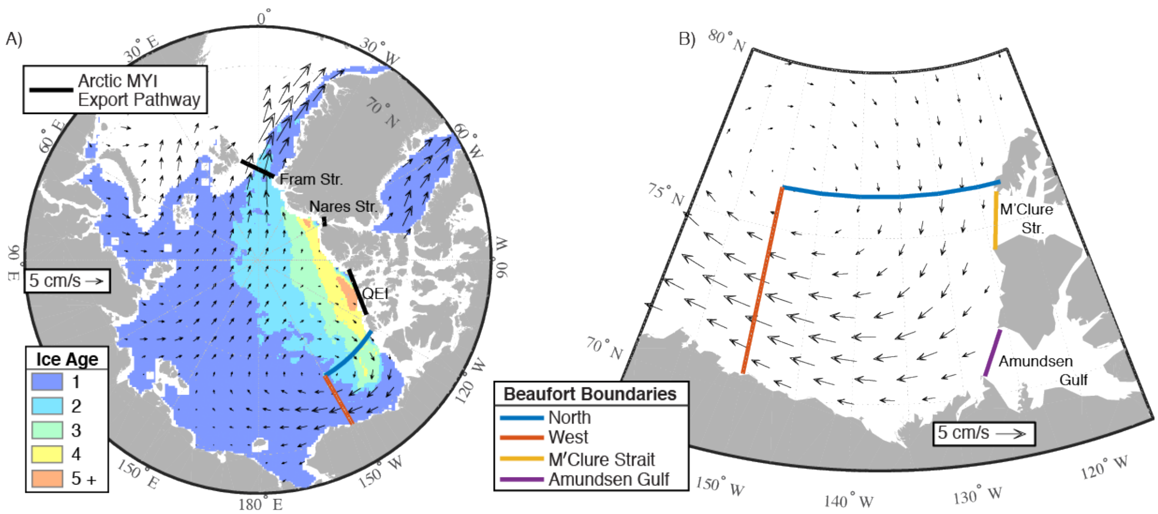

Figure 1: A) 1979-2020 mean field of sea ice motion and 2007-2020 median ice age at the end of April, with the northern and western bounds for the Beaufort Sea study region presented and the MYI export pathways marked. B) Close up of the mean field of sea ice motion through the Beaufort Sea, with the four boundaries of the Beaufort Sea study region presented. Ice Age in A) is from the NSIDC EASE-Grid Sea Ice Age v4 dataset (Tschudi et al., 2019a).

2. Methods:

To examine the MYI budget of the Beaufort Sea, the region was defined by western (150°W) and northern (76.25°N) boundaries, with two additional boundaries across Amundsen Gulf and M'Clure Strait (Figure 1B). The western and northern boundaries meet around the centre of the Beaufort Gyre, approximately enclosing its southeast quadrant (Figure 1A). The regional MYI area was calculated from weekly CIS digital ice charts and used to quantify the seasonal change in MYI area during summer (ΔMYI_S; May to the end of September) and winter (ΔMYI_W; October to the end of April). ΔMYI_W is solely the result of MYI transport across the boundaries, while a combination of MYI transport and melt dictate ΔMYI_S. Therefore, we estimate the annual area of MYI lost to melt by accounting for MYI transport. Beyond transport and melt, a small portion of MYI area may be reduced by compaction through ice deformation, however following Kwok and Cunningham (2010) this is expected to be very low and is not considered in this budget. Additionally, MYI forms locally during fall from FYI that survives through summer, which we do consider.

Ice charts delineate different ice regimes with polygons that present the partial concentrations (tenths) of up to three different stages of development according to the World Meteorological Organizations egg code (Fequet, 2005). Since 1996, ice charts are created by manually classifying these polygons in RADARSAT images. Historically, the frequency of ice charts has varied between monthly, bi-weekly and weekly intervals, though since 2007 ice charts have been produced weekly year-round. Further details on the ice charts are discussed in Galley et al., (2016) and Tivy et al., (2011).

The seasonal MYI flux (F) was calculated across the western (F_W), northern (F_N) and M'Clure (F_M) boundaries of the Beaufort Sea (Figure 1B). Amundsen Gulf was not considered in the MYI flux calculations given that during our study period it has been covered by a seasonal ice pack and the MYI pack within the Beaufort Sea was typically located west of the gate (Galley et al., 2016). Daily values of F_W and F_N were calculated at 5 km intervals across the gates:

$$F = c_{MYI}\ u\ \Delta x$$

where c_{MYI} is the MYI concentration at each point along the gate from the nearest ice chart, u is the ice velocity component normal to the gate interpolated to each point, and Δx is the distance between points (5 km). Ice velocity along the northern and western gates was extracted from the Polar Pathfinder Daily 25 km EASE-Grid Sea Ice Motion Vectors dataset (v4; Tschudi et al., 2019; updated 2021). However, the dataset does not cover the narrow channels of the CAA, hence a finer resolution sea ice motion dataset derived from sequential RADARSAT images (described in Howell & Brady, 2019 and updated through 2021) was used in conjunction with the ice charts to quantify monthly values of F_M. Note that F_M is null from November to April as landfast ice conditions in M'Clure Strait impede ice motion (Canadian Ice Service, 2011). Across all three gates positive fluxes represent ice import, while negative fluxes represent ice export from the Beaufort Sea. Cumulative seasonal ice fluxes are calculated from 1 May to 30 September for summer, and from 1 October to 30 April for winter. Lastly, the annual MYI area lost to melt is calculated as the difference between ΔMYI_S and the net summer MYI flux across all three gates.

To compliment the MYI budget, several additional datasets were used. The EASE-Grid Sea Ice Age dataset (Version 4 - Tschudi et al., 2019a) was used to provide context on the age distribution of MYI within the Beaufort Sea at the end of each winter. Unlike the CIS charts, which are manually created from RADARSAT imagery, the ice age dataset tracks lagrangian parcels of sea ice through the Polar Pathfinder ice motion dataset and counts how many years a parcel persists. The Pan-Arctic Ice-Ocean Modelling and Assimilation System (PIOMAS; Zhang & Rothrock, 2003) was used to provide estimates of ice thickness along the northern and western boundaries of the Beaufort Sea. Additionally, six-hourly fields of 2 m air temperature and surface solar radiation downwards (SSRD) were retrieved from the ERA-5 reanalysis (Copernicus Climate Change Service (C3S), 2017). SSRD was used in combination with daily fields of sea ice concentration (Cavalieri et al., 1996; updated 2021) to estimate solar heating of the upper ocean through areas of open water (F_{ow}) during summer:

$$F_{ow} = F_i(1- \alpha)\, A_{ow}$$

where F_i is the daily sum of accumulated SSRD (J m^{-2}), α is the albedo of open water (0.07) and A_{ow} is the area of open water. F_{ow} is strongly correlated with bottom melt and has been associated with both the long-term increase in bottom melt and years of anomalously high ice loss in the Beaufort Sea (Babb et al., 2016, 2019; Perovich et al., 2008, 2011; Planck et al., 2020).

3. Results and Discussion:

3.1 Regional MYI Budget

From 1997 to 2021 there has been a significant negative trend in MYI area in the Beaufort Sea at the start of May (-3,805 km^2 yr^{-1}) and end of September (-5,561 km^2 yr^{-1}; Figure 2A). The trend in September is ~35% greater than the trend in May; highlighting the tendency towards greater reductions in MYI area during summer and the continued replenishment of MYI during winter, which offsets MYI loss from the previous summer (Figure 2B). This was exemplified during the winters of 2013 and 2018 following extreme summer ice loss. Other than import, MYI is replenished by FYI surviving through summer, a process that has been fairly limited over this 25-year period (mean = 28,850 km^2) with the exception of 2013 (Figure 2B).

In terms of MYI transport, the net seasonal MYI flux varies considerably between years according to the balance of western export and northern import, with transport through M'Clure Strait accounting for only 10% of the summer MYI flux (Figure 2). During winter the average net MYI flux is an export of 4,490 km^2, but there is considerable interannual variability between import and export. For example, the net winter export peaked at 245,000 km^2 in 1998 and preconditioned the first regional sea ice minimum (Maslanik et al., 1999), while the net winter import peaked at 183,500 km^2 in 2013 and replenished MYI in the Beaufort Sea following the complete loss of the Beaufort ice pack in summer 2012 (Babb et al., 2016; Figure 2C). Underlying the variability in MYI fluxes during winter there is a significant positive trend in MYI import (+6,315 km^2 yr^{-1}) that has flipped winter from a period of MYI export at the start of the time series to a period of MYI import and replenishment more recently (Figure 2C).

During summer, an average of 47,120 km^2 of MYI is imported into the Beaufort Sea (Figure 2D). Summer export peaked at 99,430 km^2 in 1997 and contributed to the dramatic loss of MYI prior to the 1998 minimum, while net summer import peaked at 312,670 km^2 in 2018, and was solely the result of northern import. From 1997-2021, there has been a significant positive trend in northern MYI import during summer (+5,071 km^2 yr^{-1}; Figure 2D).

Overall, from 1997-2021, MYI transport through the Beaufort Sea was highly variable, but significant trends towards greater MYI import year-round have been loading MYI from the central Arctic into the Beaufort. However, less of this MYI is surviving through summer. From 1997-2021, an average of 125,000 km^2 of MYI area was lost in the Beaufort Sea each summer. The minimum loss occurred in 2017, when very little MYI was present in the Beaufort following the reversal of the Beaufort Gyre (Babb et al., 2020), while the maximum loss (385,000 km^2) occurred in 2018 (Figure 2E), though record northern import (Figure 2D) maintained a peak in regional MYI area during September 2018 (Figure 2). Between 1997-2021 there was a significant increase in MYI loss in the Beaufort Sea (-6,005 km^2 yr^{-1}; Figure

2E). The fact that the trend in MYI loss is similar to the trend in September MYI area (-5,561 $km^2\ yr^{-1}$), coupled with a non-significant trend in net MYI transport during summer, indicates that melt, not transport, is driving the increased loss of MYI in the Beaufort Sea during summer.

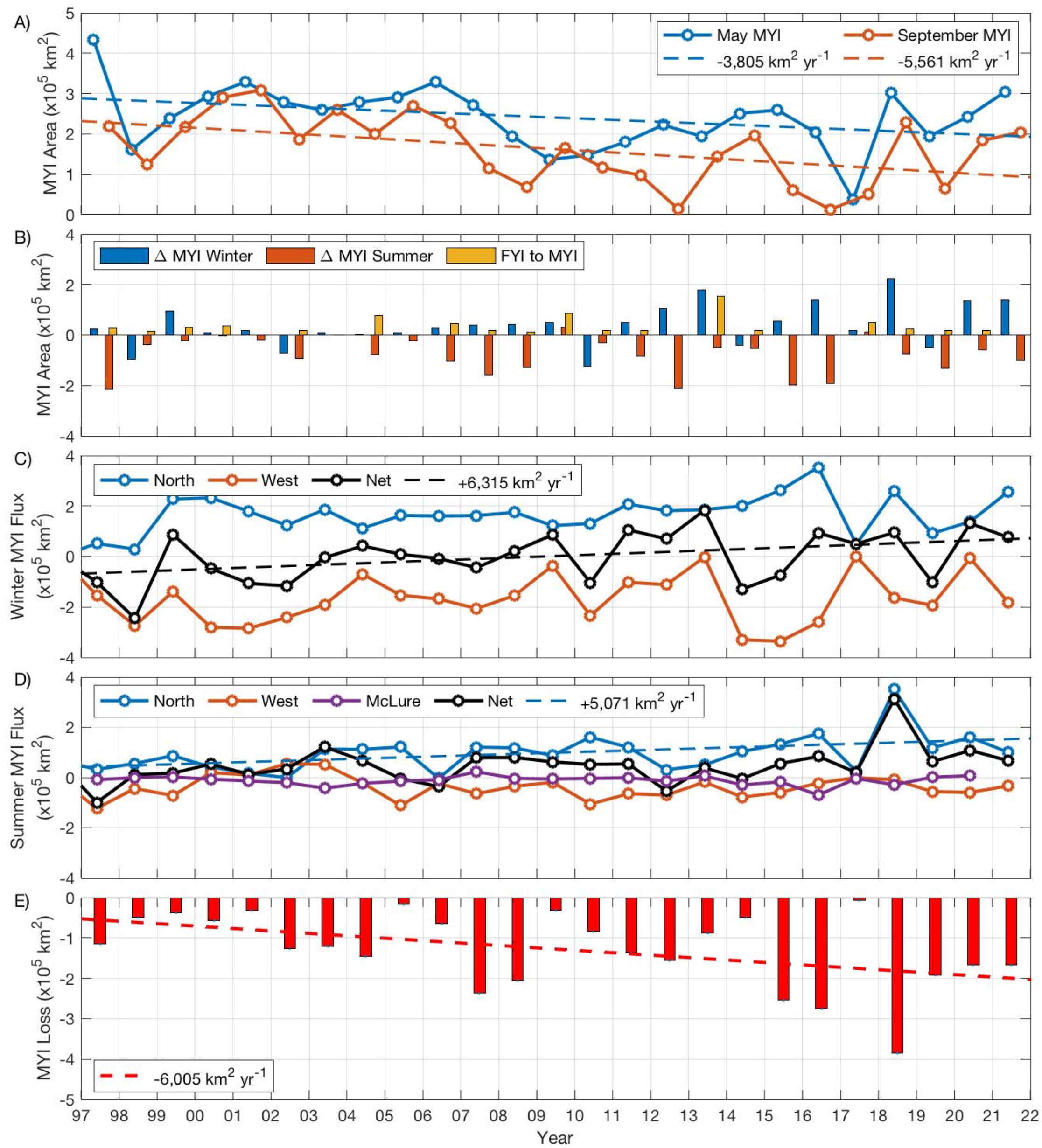

Figure 2: Annual time series of the MYI budget from 1997 to 2021. A) MYI area in the Beaufort Sea during May (blue) and September (orange). B) Seasonal changes in MYI area during winter (blue) and summer (orange), and the retention of FYI into MYI during October (yellow). MYI fluxes during winter (C) and summer (D) across the northern (blue), western (orange) and M'Clure (purple) gates, along with the net seasonal MYI flux (black). E) MYI area loss in the Beaufort Sea. Dashed lines denote significant ($p < 0.05$) trends.

3.2 Thermodynamic forcing and dynamic conditioning of MYI loss

MYI loss is not a new phenomenon in the Beaufort Sea; though between 1981 and 2005 only 7% of MYI in the western Arctic melted out each summer (Maslanik et al., 2011). The recent increase in MYI loss reflects a balance of factors that either drive ice melt (i.e. air temperatures, solar heating of the upper ocean) or dictate the condition and therefore the resiliency of the ice pack entering the melt season (i.e. thickness and age). Examining these factors over the same period as the budget reveals non-significant increases in air temperatures and solar heating of the upper ocean during summer, with notable peaks during years of regional sea ice minima (1998, 2008, 2012 and 2016; Figure 3) during which MYI loss also peaked (Figure 2E). At the same time, the presence of MYI in the Beaufort Sea has not only declined, but the age of the MYI has decreased, with a dramatic loss of MYI 5+ years old since 2010 (Figure 3C). This accompanies a significant negative trend in ice thickness along the northern gate during both winter and summer (Figure 3d). Interestingly, the peak in MYI loss during 2018 does not correspond to anomalously warm air temperatures or greater solar heating of the upper ocean during summer, but rather to an end of winter ice pack that was very young, with a majority of the MYI being only 2 years old (Figure 3). Overall, the Beaufort ice pack has been progressively conditioned towards a younger, thinner, less resilient state, while it has also been exposed to warmer air temperatures and surface waters.

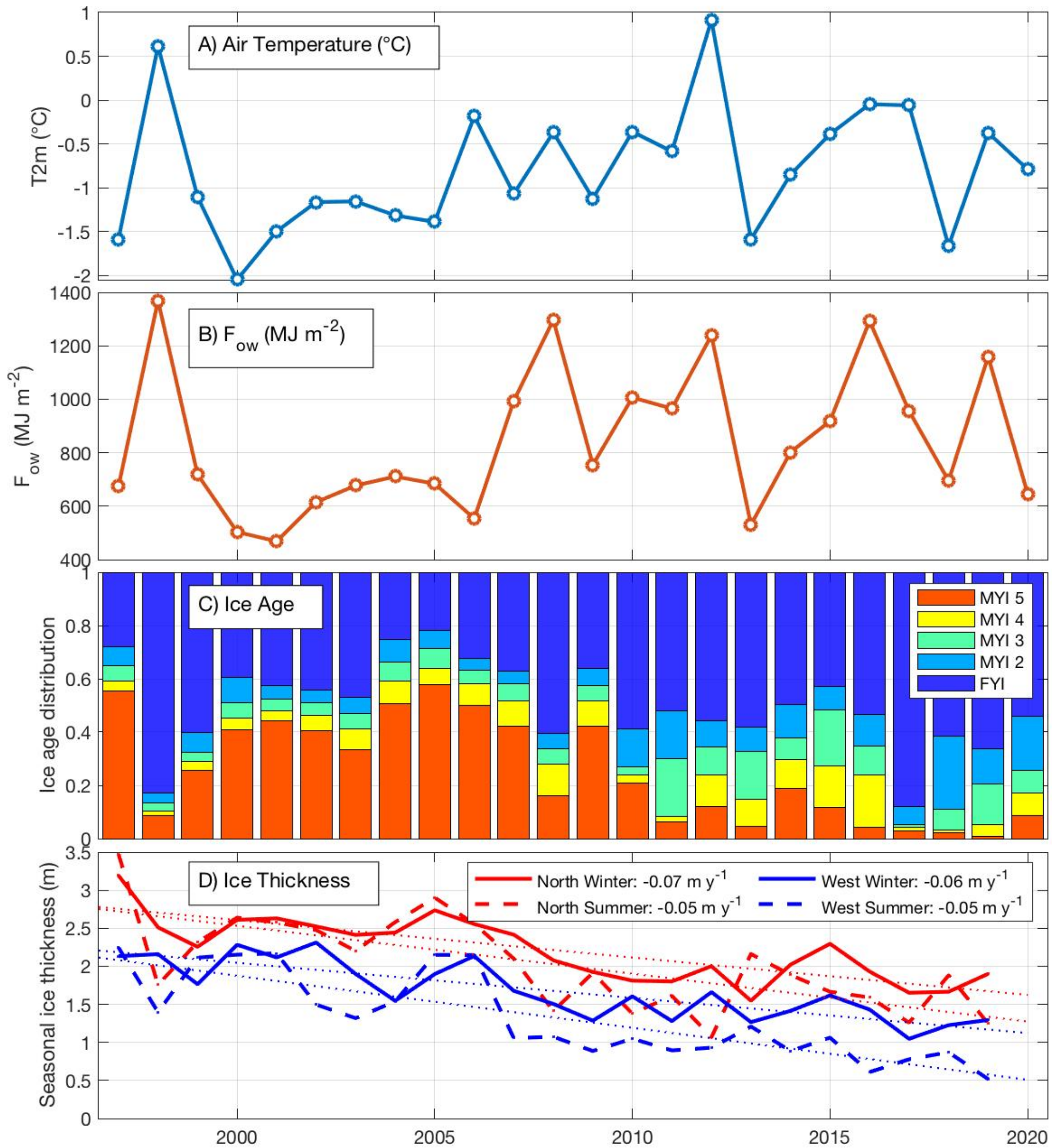

Figure 3: Time series of factors that either drive ice melt or condition the ice pack. A) Mean 2 m air temperature over the Beaufort Sea from May through September. B) Cumulative F_{ow} in the Beaufort Sea from May through September. C) Distribution of ice age within the Beaufort Sea at the end of April. D) Mean seasonal ice thickness along the northern (red) and western (blue) boundaries during winter (solid) and summer (dashed) from PIOMAS. Significant trends ($p < 0.05$) are presented with dotted lines.

3.3 Has MYI loss severed MYI transport within the Beaufort Gyre?

From 1997-2020, an average of 200,000 km^2 of MYI was exported from the Beaufort Sea across the western gate annually. However, western export is highly variable, and ranged from a maximum export of 406,000 km^2 in 2014 following the recovery of MYI in 2013, to a net import of 750 km^2 in 2017 as a result of the Beaufort Gyre reversal (Babb et al., 2020). Strong variability in MYI export precludes significant trends, although during four recent winters essentially no MYI was exported across the gate (2009, 2013, 2017 and 2020; Figure 2C). Furthermore, there is a significant positive trend in FYI export across the western gate (+11,300 km^2 yr^{-1}), indicating younger ice is being exported into the Chukchi Sea in place of MYI.

Whilst there has not been a significant trend in MYI export across the western gate, there has been a decrease in the thickness and physical character of MYI being exported across the gate. At the end of summer 2009 the remnant MYI in the western Beaufort Sea was heavily deteriorated and isothermal (Barber et al., 2009), while since 2007 remnant MYI has been so thin that by the end of the following winter it is as thick as the surrounding FYI (Mahoney et al., 2019). Furthermore, there is also significant negative trend in sea ice thickness along the western gate during summer and winter (Figure 3).

MYI transport from the Beaufort Sea into the Chukchi Sea as part of the Beaufort Gyre has not been totally severed. However, reductions in the area, thickness and age of MYI transported through the Beaufort Sea into the Chukchi Sea have created an ice pack in the Pacific sector of the Arctic that is less resilient to warm pacific waters flowing through the Bering Strait (Woodgate et al., 2010) and the subsequent ice-albedo feedback (Serreze et al., 2016) that are collectively driving ice loss in this area.

3.4 Has the Beaufort Sea become an area of MYI export?

Traditionally, MYI export occurs along the boundaries of the Arctic Ocean and represents the total loss of MYI. Fram Strait is the primary export pathway (Kwok, 2009) exporting between 450,000 and 660,000 km^2 of MYI annually (Table 1). MYI is also exported annually through Nares Strait and into the QEI (Howell & Brady, 2019; Kwok, 2005, 2006; Moore et al., 2021), and has occasionally been exported into the Barents Sea (Kwok, 2004) and through the Bering Strait (Babb et al., 2013). To define the Beaufort Sea as an export pathway similar to these other locations the regional MYI pack would have to be completely lost. This has happened three times during the last decade (2010, 2012, 2016), but as we have just shown MYI, albeit a younger and thinner form of MYI does continue to be advected downstream within the Gyre. Hence, the Beaufort Sea has not completely become an export pathway, but it increasingly resembles one.

Comparing MYI loss in the Beaufort to MYI export through the traditional export pathways reveals that during the first pentad of our budget (1997-2001) MYI loss in the Beaufort was approximately twice the net MYI export through Nares Strait and into the QEI, but only 6% to 9% of the MYI export through Fram Strait (Table 1). Comparatively, during the most recent pentad (2017-2021) MYI loss in the Beaufort Sea was approximately three times the net MYI export through Nares Strait and into the QEI, and approximately 27% to 40% of the annual MYI export through Fram Strait (Table 1). Furthermore, the 2018 peak in MYI loss (385,000 km^2) was close to the conservative estimate of MYI export through Fram Strait.

Without estimates of MYI loss in other regions it is not possible to compare sub-regional MYI loss to the overall pan-Arctic annual MYI loss (melt + export). Although this comparison shows that amongst these four pathways of MYI loss, the Beaufort Sea continues to have the second greatest magnitude, and that its relative contribution to the Arctic MYI balance has significantly increased. This increase is critical for the MYI that remains along northern Greenland and the CAA, as it is now bookended by Fram Strait and the Beaufort Sea (Figure 1A) and is susceptible to being lost through either side. Historically, MYI advected from the central Arctic through the Beaufort Gyre was conserved, particularly during years with a strong Beaufort High (negative AO; Rigor & Wallace, 2002; Stroeve et al., 2011). However, increasing ice melt in the Beaufort makes it unlikely that MYI advected out of the Central Arctic will survive through the Beaufort Sea, or will be heavily deteriorated by the time it reaches the Chukchi Sea, and thereby limits the potential of a strong Beaufort High from facilitating the redistribution and recovery of MYI. As an example, during winter 2021 a strong Beaufort High advected MYI out of the central Arctic into the Beaufort Sea (Mallett et al., 2021), and while this facilitated a slight recovery in the time series of the regional MYI area (Figure 2A), over 170,000 km^2

of this MYI was lost (Figure 2E) and we speculate that the remaining MYI experienced considerable melt.

Ultimately, the combination of increasing MYI loss in the Beaufort Sea (Figure 2E), increasing MYI export through Nares Strait (Moore et al., 2021) and into the QEI (Howell & Brady, 2019), and continued MYI export through Fram Strait is depleting the reservoir of MYI in the Arctic Ocean, a trend which is compounded by a concomitant decrease in MYI replenishment by FYI (Kwok, 2007). The imbalance between MYI loss and FYI replenishment is being amplified by increasing MYI loss in the Beaufort Sea, and is driving the transition to a predominantly seasonal ice cover that is inherently thinner and will eventually lead to the occurrence of a seasonally ice-free Arctic around the middle of this century (SIMIP, 2020).

Table 1: Comparison of MYI loss in the Beaufort Sea to MYI export across the boundaries of the Arctic Ocean.

	Years			**Annual MYI loss**
MYI loss in the Beaufort Sea	1997-2001			42,360 km^2
	2017-2021			183,250 km^2
Export Pathway	**Years**	**Annual ice export**	**Proportion MYI**	**Annual MYI loss**
Fram Strait	1979-2007	706,000 km^2 [a]	64-94% [b]	451,000 – 663,000 km^2
Nares Strait	1996-2002	33,000 km^2 [c]	50% [c]	16,500 km^2
	2019-2021	87,000 km^2 [d]	50% [c]	43,500 km^2
QEI	1997-2002	8,000 km^2 [e]	100%*	8,000 km^2
	1997-2018	25,000 km^2 [f]	100%*	25,000 km^2

Notes: [a] – Kwok (2009); [b] – Ricker et al., (2018); [c] – Kwok, (2005); [d] – Moore et al., (2021); [e] – Kwok, (2006); [f] – Howell et al., (2019).
* Assumed based on the CIS ice charts.

3.5 The impacts of increasing MYI loss in the Beaufort Sea

The loss of MYI has various impacts on the way that humans and wildlife interact with the ice pack within the Beaufort Sea. Given its thickness, and strength, MYI represents a considerable hazard to vessels operating in ice-covered waters. The reduction in MYI area within the Beaufort Sea corresponds to an increase in shipping activity (Pizzolato et al., 2016), particularly pleasure craft that are accessing the Northwest Passage (Dawson et al., 2018). Shipping in the Beaufort Sea is proposed to continue to increase as the shipping season length continues to increase (Mudryk et al., 2021). However, the continued replenishment of MYI during winter will maintain some level of risk associated with hazardous ice (Barber et al., 2014).

The transition to a thinner seasonal ice pack is projected to increase productivity in the Arctic (Tedesco et al., 2019) and has been proposed to offer some short-term benefits to Polar Bears (Derocher et al., 2004). However, Laidre et al., (2020) noted that this has yet to be demonstrated and suggest any advantage may only be temporary before the negative effects of climate change (i.e. habitat loss) begin to outweigh any potential positives. Historically, Polar Bears within the Beaufort Sea retreated to the MYI pack during summer (Derocher et al., 2004) and even denned on MYI floes during winter (Amstrup & Gardner, 1994). But MYI loss (Figure 2E) combined with the northern retreat of the MYI edge (Galley et al., 2016), is both removing and fragmenting this habitat and increasing the distance that bears may need to swim to reach either the remaining MYI or land (Pagano et al., 2021).

4. Conclusions:

Historically, the Beaufort Sea served as a conduit for MYI transport from the central Arctic to the Eastern Arctic through the Beaufort Gyre, and thereby facilitated the presence of MYI throughout much of the Arctic Ocean. However, increasing ice melt during the early-2000s led Maslanik et al. (2007) to propose that the Beaufort Sea had become an area of MYI export and that MYI transport through the Beaufort Gyre had been severed. Using a regional MYI budget from 1997-2021, we have determined that MYI transport through the Beaufort Sea has not been completely severed, but that it has been interrupted and essentially now provides no replenishment of MYI to the Eastern Arctic. The budget reveals that MYI import into the Beaufort Sea has increased during both summer and winter, but that less of this MYI now survives through summer. Over the 25-year study period, MYI area loss increased at 6,289 km^2 yr^{-1}, nearly quadrupling the annual mean area of MYI lost from 42,360 km^2 between 1997-2001 to 183,000 km^2 between 2017-2021. MYI area loss peaked at 385,000 km^2 in 2018.

Historically, the pan-Arctic MYI budget was dominated by MYI loss through Fram Strait. At the start of the record, MYI loss in the Beaufort Sea represented only 7% of the annual MYI export through Fram Strait. However, from 2017-2021 this increased to ~35%, with the peak in 2018 matching the conservative estimate of MYI export through Fram Strait (~400,000 km^2). This increase in MYI loss in the Beaufort Sea has been driven by a combination of thermodynamic forcing and dynamic conditioning, which have collectively exposed a younger, thinner ice pack to warmer air temperatures and a warmer ocean. Increased MYI loss has interrupted MYI transport through the Gyre, leading to a deteriorated form of MYI being advected downstream and thereby affecting the state of the Chukchi Sea ice pack. Ultimately, the contribution of MYI loss in the Beaufort Sea to the overall MYI budget of the Arctic Ocean has dramatically increased and is a key driver of the transition to a seasonal Arctic ice pack.

Acknowledgements:

D. Babb, R. Galley and D. Barber would like to acknowledge the financial support from the Natural Sciences and Engineering Research Council of Canada (NSERC). Thanks to the Canada Research Chairs (CRC), Canada Excellence Research Chair (CERC) and the Canada-150 (C-150) Chair programs. D. Babb acknowledges the financial support from the Canadian Meteorological and Oceanographic Society (CMOS). J. Landy acknowledges support from the Centre for Integrated Remote Sensing and Forecasting for Arctic Operations (CIRFA) project through the Research Council of Norway (RCN) under Grant #237906. J. Landy and J. Stroeve acknowledge support from the Natural Environment Research Council Project "PRE-MELT" under Grant NE/T000546/1. We would also like to thank the editor and reviewers for their help in improving this manuscript.

Data Availability

CIS ice charts are freely available online (https://www.canada.ca/en/environment-climate-change/services/ice-forecasts-observations.html). The NSIDC ice motion (https://nsidc.org/data/nsidc-0116/versions/4) and ice age (https://nsidc.org/data/NSIDC-0611/versions/4) datasets are available online. PIOMAS Ice thickness data is available online (http://psc.apl.uw.edu/research/projects/arctic-sea-ice-volume-anomaly/data/model_grid). ERA5 atmospheric reanalysis products are available from the Climate Data Store through the Copernicus Climate Change Service (https://cds.climate.copernicus.eu/cdsapp#!/dataset/reanalysis-era5-single-levels?tab=overview).

References:

Amstrup, S. C., & Gardner, C. L. (1994). Polar bear maternity denning in the Beaufort Sea. *Journal of Wildlife Management*, *58*(1), 1–10. https://doi.org/10.2307/3809542

Babb, D.G., Landy, J. C., Lukovich, J. V., Haas, C., Hendricks, S., Barber, D. G., & Galley, R. J. (2020). The 2017 reversal of the Beaufort Gyre: Can dynamic thickening of a seasonal ice cover during a reversal limit summer ice melt in the Beaufort Sea? *Journal of Geophysical Research: Oceans*, 1–26. https://doi.org/10.1029/2020jc016796

Babb, David G., Galley, R. J., Asplin, M. G., Lukovich, J. V., & Barber, D. G. (2013). Multiyear sea ice export through the Bering Strait during winter 2011-2012. *Journal of Geophysical Research: Oceans*, *118*(10), 5489–5503. https://doi.org/10.1002/jgrc.20383

Babb, David G., Galley, R. J., Barber, D. G., & Rysgaard, S. (2016). Physical processes contributing to an ice free Beaufort Sea during September 2012. *Journal of Geophysical Research: Oceans*, *121*, 267–283. https://doi.org/10.1002/2015JC010756

Babb, David G., Landy, J. C., Barber, D. G., & Galley, R. J. (2019). Winter Sea Ice Export From the Beaufort Sea as a Preconditioning Mechanism for Enhanced Summer Melt: A Case Study of 2016. *Journal of Geophysical Research: Oceans*, *1998*(6575), 6575–6600. https://doi.org/10.1029/2019JC015053

Barber, D. G., Galley, R. J., Asplin, M. G., De Abreu, R., Warner, K. A., Pučko, M., et al. (2009). Perennial pack ice in the southern beaufort sea was not as it appeared in the summer of 2009. *Geophysical Research Letters*, *36*(24), 1–5. https://doi.org/10.1029/2009GL041434

Barber, D. G., McCullough, G., Babb, D. G., Komarov, A., Candlish, L. M., Lukovich, J. V., et al. (2014). Climate change and ice hazards in the Beaufort Sea. *Elementa: Science of the Anthropocene*, *2*(1982), 000025. https://doi.org/10.12952/journal.elementa.000025

Bourke, R. H., & Garret, R. P. (1987). Sea ice thickness distribution in the Arctic Ocean. *Cold Regions Science and Technology*, *13*, 259–280.

Canadian Ice Service. (2011). *Sea Ice Climatic Atlas for the Northern Canadian Waters 1981-2011*. Ottawa, Canada.

Cavalieri, D. J., Parkinson, C. L., Gloersen, P., & Zwally, H. J. (1996). *Sea Ice Concentrations from Nimbus-7 SMMR and DMSP SSM/I-SSMIS PAssive Microwave Data*. Boulder, Colorado, USA.

Copernicus Climate Change Service (C3S). (2017). ERA5: Fifth generation of ECMWF atmospheric reanalysis of the global climate. Copernicus Climate Change Service Climate Data Store.

Dawson, J., Pizzolato, L., Howell, S. E. L., Copland, L., & Johnston, M. E. (2018). Temporal and Spatial Patterns of Ship Traffic in the Canadian Arctic from 1990 to 2015 + Supplementary Appendix 1: Figs. S1–S7 (See Article Tools). *Arctic*, *71*(1), 15. https://doi.org/10.14430/arctic4698

Derocher, A. E., Lunn, N. J., & Stirling, I. (2004). Polar Bears in a Warming Climate. *Integrative and Comparative Biology*, *44*(2), 163–176.

https://doi.org/10.1093/icb/44.2.163

Fequet, D. (2005). *Manual of Standard Procedures for Observing and Reporting Ice Conditions* (9th ed.). Ottawa: Canadian Ice Service, Environment Canada.

Galley, R. J., Babb, D. G., Ogi, M., Else, B. G. T., Geifus, N. X., Crabeck, O., et al. (2016). Replacement of multiyear sea ice and changes in the open water season duration in the Beaufort Sea since 2004. *Journal of Geophysical Research: Oceans*, *121*(April), 1–18. https://doi.org/10.1002/2015JC011583.Received

Howell, S. E. L., & Brady, M. (2019). The Dynamic Response of Sea Ice to Warming in the Canadian Arctic Archipelago. *Geophysical Research Letters*, *46*(22), 13119–13125. https://doi.org/10.1029/2019GL085116

Howell, S. E. L., Brady, M., Derksen, C., & Kelly, R. E. J. (2016). Recent changes in sea ice area flux through the Beaufort Sea during the summer. *Journal of Geophysical Research: Oceans*, *121*, 1–14. https://doi.org/10.1002/2015JC011464

Hutchings, J. K., & Rigor, I. G. (2012). Role of ice dynamics in anomalous ice conditions in the Beaufort Sea during 2006 and 2007. *Journal of Geophysical Research: Oceans*, *117*(5), 1–14. https://doi.org/10.1029/2011JC007182

Krishfield, R. A., Proshutinsky, A., Tateyama, K., Williams, W. J., Carmack, E. C., McLaughlin, F. A., & Timmermans, M.-L. (2014). Deterioration of perennial sea ice in the Beaufort Gyre from 2003 to 2012 and its impact on the oceanic freshwater cycle. *Journal of Geophysical Research: Oceans*, *119*, 35. https://doi.org/10.1002/2013JC008999

Kwok, R. (2004). Fram Strait sea ice outflow. *Journal of Geophysical Research*, *109*(C1), C01009. https://doi.org/10.1029/2003JC001785

Kwok, R. (2005). Variability of Nares Strait ice flux. *Geophysical Research Letters*, *32*(24), 1–4. https://doi.org/10.1029/2005GL024768

Kwok, R. (2006). Exchange of sea ice between the Arctic Ocean and the Canadian Arctic Archipelago. *Geophysical Research Letters*, *33*(16), 1–5. https://doi.org/10.1029/2006GL027094

Kwok, R. (2007). Near zero replenishment of the Arctic multiyear sea ice cover at the end of 2005 summer. *Geophysical Research Letters*, *34*(5), 1–6. https://doi.org/10.1029/2006GL028737

Kwok, R. (2009). Outflow of Arctic Ocean sea ice into the Greenland and Barent Seas: 1979-2007. *Journal of Climate*, *22*(9), 2438–2457. https://doi.org/10.1175/2008JCLI2819.1

Kwok, R. (2015). Sea ice convergance along the Arctic coasts of Greenland and the Canadian Arctic Archipelago: Variability and extremes (1992-2014). *Geophysical Research Letters*, *42*, 1–8. https://doi.org/10.1002/2015GL065462

Kwok, R. (2018). Arctic sea ice thickness, volume , and multiyear ice coverage: losses and coupled variability (1958 – 2018). *Environmental Research Letters*, *13*(10), 105005. https://doi.org/10.1088/1748-9326/aae3ec

Kwok, R., & Cunningham, G. F. (2010). Contribution of melt in the Beaufort Sea to the decline in Arctic multiyear sea ice coverage: 1993-2009. *Geophysical Research Letters*, *37*(20), 1–5. https://doi.org/10.1029/2010GL044678

Laidre, K. L., Atkinson, S. N., Regehr, E. V, Stern, H. L., Born, E. W., Wiig, Ø., et al. (2020). Transient benefits of climate change for a high-Arctic polar bear (Ursus maritimus) subpopulation. *Global Change Biology*, *26*(11), 6251–6265. https://doi.org/https://doi.org/10.1111/gcb.15286

Mahoney, A. R., Hutchings, J. K., Eicken, H., & Haas, C. (2019). Changes in the Thickness and Circulation of Multiyear Ice in the Beaufort Gyre Determined From Pseudo-Lagrangian Methods from 2003–2015. *Journal of Geophysical Research: Oceans*, *124*(8), 5618–5633. https://doi.org/10.1029/2018JC014911

Mallett, R. D. C., Stroeve, J. C., Cornish, S. B., Crawford, A. D., Lukovich, J. V., Serreze, M. C., et al. (2021). Record winter winds in 2020/21 drove exceptional Arctic sea ice transport. *Communications Earth & Environment*, *2*(1), 17–22. https://doi.org/10.1038/s43247-021-00221-8

Maslanik, J. A., Serreze, M. C., & Agnew, T. (1999). On the record reduction in 1998 Western Arctic sea-ice cover. *Geophysical Research Letters*, *26*(13), 1905–1908. https://doi.org/10.1029/1999GL900426

Maslanik, J. A., Fowler, C., Stroeve, J. C., Drobot, S., Zwally, J., Yi, D., & Emery, W. (2007). A younger, thinner Arctic ice cover: Increased potential for rapid, extensive sea-ice loss. *Geophysical Research Letters*, *34*(24), 2004–2008. https://doi.org/10.1029/2007GL032043

Maslanik, J. A., Stroeve, J. C., Fowler, C., & Emery, W. (2011). Distribution and trends in Arctic sea ice age through spring 2011. *Geophysical Research Letters*, *38*(13), 2–7. https://doi.org/10.1029/2011GL047735

Moore, G. W. K., Howell, S. E. L., Brady, M., Xu, X., & McNeil, K. (2021). Anomalous collapses of Nares Strait ice arches leads to enhanced export of Arctic sea ice. *Nature Communications*, *12*(1), 1–8. https://doi.org/10.1038/s41467-020-20314-w

Mudryk, L. R., Dawson, J., Howell, S. E. L., Derksen, C., Zagon, T. A., & Brady, M. (2021). Impact of 1, 2 and 4 °C of global warming on ship navigation in the Canadian Arctic. *Nature Climate Change*, 29–31. https://doi.org/10.1038/s41558-021-01087-6

Nghiem, S. V., Chao, Y., Neumann, G., Li, P., Perovich, D. K., Street, T., & Clemente-Colón, P. (2006). Depletion of perennial sea ice in the East Arctic Ocean. *Geophysical Research Letters*, *33*(17), 1–6. https://doi.org/10.1029/2006GL027198

Nghiem, S. V., Rigor, I. G., Perovich, D. K., Clemente-Colón, P., Weatherly, J. W., & Neumann, G. (2007). Rapid reduction of Arctic perennial sea ice. *Geophysical Research Letters*, *34*(19), 1–6. https://doi.org/10.1029/2007GL031138

Pagano, A. M., Durner, G. M., Atwood, T. C., & Douglas, D. C. (2021). Effects of sea ice decline and summer land use on polar bear home range size in the Beaufort Sea. *Ecosphere*, *12*(10). https://doi.org/10.1002/ecs2.3768

Perovich, D. K., Richeter-Menge, J. A., Jones, K. F., & Light, B. (2008). Sunlight, water, and ice: Extreme Arctic sea ice melt during the summer of 2007. *Geophysical Research Letters*, *35*(11), 2–5. https://doi.org/10.1029/2008GL034007

Perovich, D. K., Richter-Menge, J. A., Jones, K. F., Light, B., Elder, B. C., Polashenski, C., et al. (2011). Arctic sea-ice melt in 2008 and the role of solar heating. *Annals of Glaciology*, *52*(57 PART 2), 355–359. https://doi.org/10.3189/172756411795931714

Pizzolato, L., Howell, S. E. L., Dawson, J., Laliberté, F., & Copland, L. (2016). The influence of declining sea ice on shipping activity in the Canadian Arctic. *Geophysical Research Letters*, *43*(23), 12,146-12,154. https://doi.org/10.1002/2016GL071489

Planck, C. J., Perovich, D. K., & Light, B. (2020). A Synthesis of Observations and Models to Assess the Time Series of Sea Ice Mass Balance in the Beaufort Sea. *Journal of Geophysical Research: Oceans*, 1–15. https://doi.org/10.1029/2019jc015833

Ricker, R., Girard-Ardhuin, F., Krumpen, T., & Lique, C. (2018). Satellite-derived sea ice export and its impact on Arctic ice mass balance. *The Cryosphere*, *12*(9), 3017–3032. https://doi.org/10.5194/tc-12-3017-2018

Rigor, I. G., & Wallace, J. M. (2002). Response of sea ice to the Arctic Oscillation. *Applied Physics*, 2648–2663. https://doi.org/10.1175/1520-0442(2002)015<2648:ROSITT>2.0.CO;2

Rigor, I. G., & Wallace, J. M. (2004). Variations in the age of Arctic sea-ice and summer sea-ice extent. *Geophysical Research Letters*, *31*(9), 2–5. https://doi.org/10.1029/2004GL019492

Serreze, M. C., Crawford, A. D., Stroeve, J. C., Barrett, A. P., & Woodgate, R. A. (2016). Variability, trends, and predictability of seasonal sea ice retreat and advance in the Chukchi Sea. *Journal of Geophysical Research: Oceans*, *121*, 7308–7325. https://doi.org/10.1002/2016JC011977

SIMIP Community. (2020). Arctic Sea Ice in CMIP6. *Geophysical Research Letters*, *47*(10). https://doi.org/10.1029/2019gl086749

Stroeve, J. C., Maslanik, J. A., Serreze, M. C., Rigor, I. G., Meier, W., & Fowler, C. (2011). Sea ice response to an extreme negative phase of the Arctic Oscillation during winter 2009/2010. *Geophysical Research Letters*, *38*(2), 1–6. https://doi.org/10.1029/2010GL045662

Tedesco, L., Vichi, M., & Scoccimarro, E. (2019). Sea-ice algal phenology in a warmer Arctic. *Science Advances*, *5*(5). https://doi.org/10.1126/sciadv.aav4830

Tivy, A., Howell, S. E. L., Alt, B., McCourt, S., Chagnon, R., Crocker, G., et al. (2011). Trends and variability in summer sea ice cover in the Canadian Arctic based on the Canadian Ice Service Digital Archive, 1960-2008 and 1968-2008. *Journal of Geophysical Research: Oceans*, *116*(3). https://doi.org/10.1029/2009JC005855

Tschudi, M. A., Meier, W. N., Stewart, J. S., Fowler, C., & Maslanik, J. A. (2019a). *EASE-Grid Sea Ice Age, Version 4*. Boulder, Colorado, USA. https://doi.org/https://doi.org/10.5067/UTAV7490FEPB

Tschudi, M. A., Meier, W. N., Stewart, J. S., Fowler, C., & Maslanik, J. A. (2019b). *Polar Pathfinder Daily 25 km EASE-Grid Sea Ice Motion Vectors, Version 4*. Boulder, Colorado, USA. https://doi.org/https://doi.org/10.5067/INAWUWO7QH7B

Woodgate, R. A., Weingartner, T., & Lindsay, R. (2010). The 2007 Bering Strait oceanic heat flux and anomalous Arctic sea-ice retreat. *Geophysical Research Letters*, *37*(1), 1–5. https://doi.org/10.1029/2009GL041621

Zhang, J., & Rothrock, D. A. (2003). Modeling global sea ice with a thickness and enthalpy distribution model in generalized curvilinear coordinates. *Monthly Weather Review*, *131*(5), 845–861. https://doi.org/10.1175/1520-0493(2003)131<0845:MGSIWA>2.0.CO;2